Inter-Layer Energy Transfer through Wetting-Layer States in Bi-layer InGaAs/GaAs Quantum-Dot Structures with Thick Barriers

Xu, Zhang-Cheng; Zhang, Ya-Ting; Hvam, Jørn Märcher; Horikoshi, Yoshiji

Published in:
Chinese Physics Letters

Link to article, DOI:
10.1088/0256-307X/26/5/057304

Publication date:
2009

Document Version
Early version, also known as pre-print

Vertical Carrier Transfer in Asymmetric Bilayer of InGaAs/GaAs Quantum Dots

Zhangcheng Xu and Yating Zhang
Key Laboratory of Advanced Technique and Fabrication for Weak-Light Nonlinear Photonics Material (Ministry of Education), TEDA College, Nankai University, Tianjin 300457, People's Republic of China

Jørn M. Hvam
Department of Communications, Optics and Materials, and Nano.DTU, Technical University of Denmark, DK-2800 Lyngby, Denmark

(Dec. 31, 2006)

Vertical carrier transfer in asymmetric InGaAs/GaAs quantum dot (QD) pairs is studied via time-resolved photoluminescence (PL) spectroscopy. From the correlation between the height distribution and the PL line-shape of the QD ensembles, the tunneling time is found as a function of barrier thickness, in good agreement with the Wentzel-Kramers-Brillouin approximation. The tunneling rates for vertically coupled QDs are comparable to those of coupled quantum wells, indicating that carrier tunneling occurs from the discrete states of the QDs in the layer with lower coverage to the quasi-continuum states of the QDs in the layer with higher coverage, via LO phonon emission.

Growth and device applications of semiconductor quantum dots (QDs) have received much attention recently[1,2,3]. InGaAs/GaAs QDs with high density and good crystal quality can be epitaxially grown using molecular beam epitaxy (MBE) or metalorganic vapor phase epitaxy (MOCVD). Stacking the QDs with thin barriers can be used to tune the volume density and the emission wavelength[4], to fulfill the device requirements. When the barriers are thin enough in the stacked QD system, the carrier tunneling transfer becomes significant, which was previously studied by various authors.[5,6,7,8] However, their results on the barrier thickness dependence of the transfer time are quite different from each other.

In this paper, we present a new way of elucidating the dependence of carrier tunneling time on the effective barrier thickness, based on the correlation of the distribution of QD heights and the emission energies in the bottom layer of QDs in an asymmetric bilayer of InGaAs/GaAs QDs.

Two samples were grown using MBE on semi-insulating GaAs (100) substrates. The layer structure of Sample No.1 is shown in Figure 1a. It contains two layers of buried $In_{0.6}Ga_{0.4}As$ QDs (QD1 and QD 2) and one layer of surface $In_{0.6}Ga_{0.4}As$ QDs (QD3), grown via Stranski-Kristanow (SK) mode. QD1 and QD3 are formed by depositing 5 monolayers (MLs) of $In_{0.6}Ga_{0.4}As$, while 7MLs are deposited for QD2. Sample No.2 contains only one layer of buried 5-ML $In_{0.6}Ga_{0.4}As$ QDs, as a reference. For optical characterizations, the surface QDs (QD3) of Sample No.1 was removed.

Figure 1b shows the $400 \times 400 nm^2$ atomic force microscopy (AFM) image of QD3. The number density of the SQDs is estimated to be $7.5 \times 10^{10} cm^{-2}$. Figure 1c shows a histogram of the height statistics of QD3, which can be well fitted by a single Gaussian distribution function with the maximum number of QDs at $Height_{mean} = 3.2nm$ and full width at half maximum (FWHM), $FWHM_{Height} = 3.3nm$. Note that the actual distances between the vertical adjacent QDs in QD1 and QD2 are modulated by the height fluctuation of QDs in QD1, although the nominal thickness of the GaAs spacer between QD1 and QD2 is 17 nm. This is confirmed in the case of the stacked InAs/GaAs QDs.[4,8]

Figure 2 shows the X-ray rocking curve of Sample No.1 around the GaAs (0 0 4) reflection peak, which was measured by using a Rigaku RINT-TTR X-ray diffractometer. The fitting curve was calculated by using the Takagi-Taupin equation and assuming that the QD layers are tetragonally distorted quantum wells[9,10]. It can be seen that the calculated curve agrees well with the experimental one, except for some discrepancy in a few fringe positions due to non-uniformity of QDs.

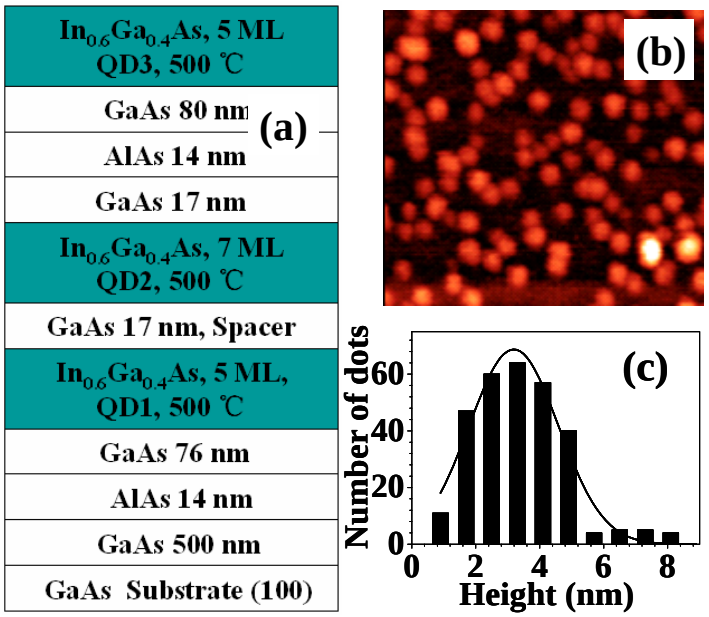

Figure 1 (a) Schematic of the layer structure of Sample No.1. (b) $400 \times 400 nm^2$ AFM image of the surface QDs (QD3). (b) Histogram of the height of the surface QDs.

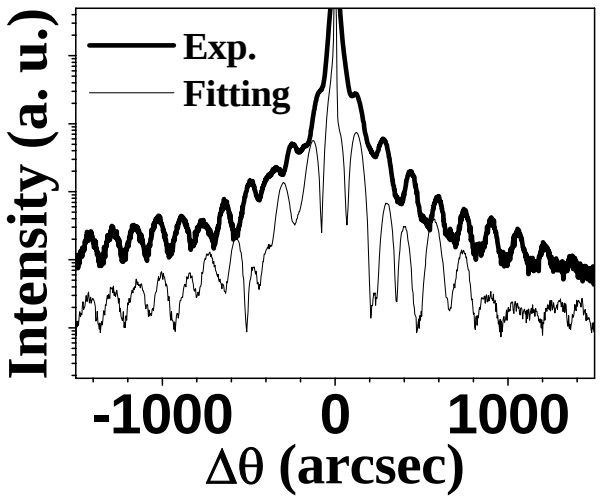

Figure 2 X-ray rocking curve of Sample No.1 around GaAs (0 0 4) peak.

Time-resolved PL measurements were carried out using 130 fs pulses at $\lambda = 800nm$ from a mode-locked Ti:Sapphire laser with a repetition rate of 76 MHz . A monochromator and a synchro-scan streak camera with a time resolution of 2.5 ps are used to detect the PL signal. The details of the experiments can be seen in Refs. 11 and 12. The samples are cooled in a liquid-helium cryostat, at 5 K. An excitation density of 1×10^9 $photons/(pulse \times cm^2)$ is chosen to get sufficiently high signal-to-noise ratios and still avoid excited-state PL contributions.

The PL spectrum for the reference sample (Sample No..2) at 500 ps after the laser

pulse, is shown in Figure 3a. The PL peak can be well fitted using a Gaussian at $E_{R,\max} = 1.336eV$ with $FWHM_R = 40.5meV$. Figure 3b shows the PL transients at three different detection energies, which can be well fitted mono-exponentially, giving the PL decay time τ_d. The spectral dependence of the PL decay time is plotted with solid squares in Figure 3a. It can be seen that τ_d increases slightly from 934 ps to 1398 ps, as the emission energy decreases from 1.368 eV to 1.307 eV. This behavior is typical of a dense array of QDs, in which carriers tunnel from the ground states of smaller QDs to the ground state of larger QDs[14].

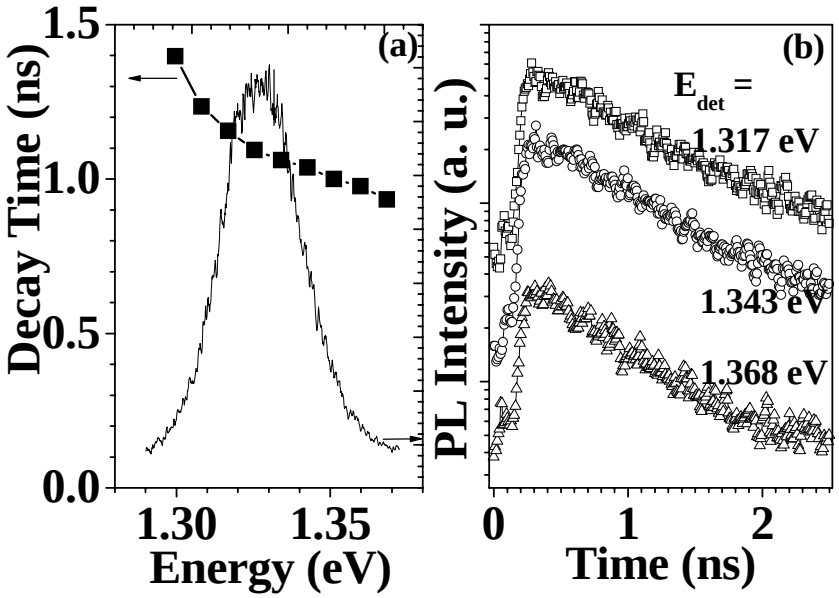

Figure 3 (a) PL spectrum and spectral dependence of the PL decay time in InGaAs/GaAs quantum dot structure at 5 K. (b) PL transient measure at different detection energies.

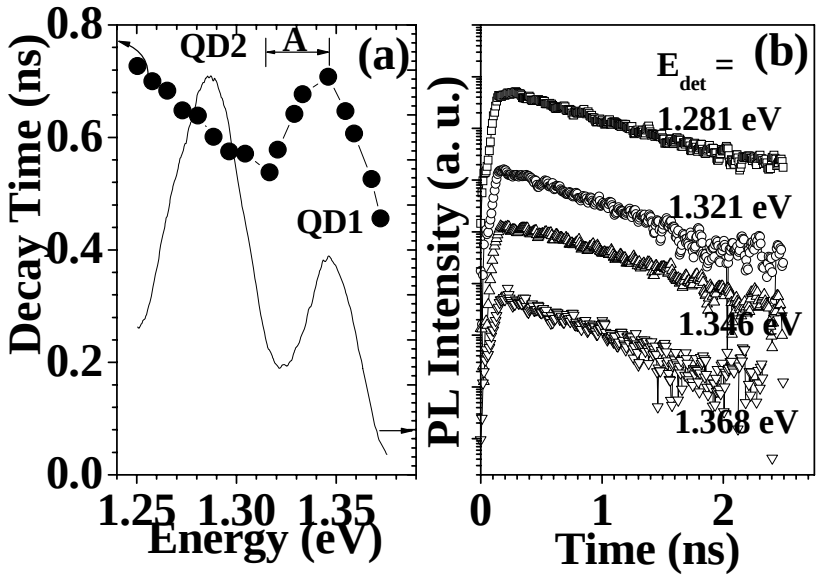

Fig. 4 (a) PL spectrum and spectral dependence of the PL decay time in InGaAs/GaAs asymmetric bilayer quantum dot structure at 5 K. (b) PL transient measure at different detection energies.

Figure 4a shows the PL spectrum, for the asymmetric bilayer InGaAs/GaAs quantum dot structure (Sample No.1), at 500 ps after the excitation pulse. Two peaks can be clearly seen and fitting the spectrum with two Gaussians gives one peak at $E_{1,\max} = 1.347eV$ with $FWHM_1 = 28.9meV$ and the other at $E_{2,\max} = 1.284eV$ with $FWHM_2 = 56.4meV$, which correspond to the first layer of QDs (QD1) and the second layer of QDs (QD2), respectively. The higher peak energy and the narrower PL line-width for QD1 than the reference QD sample (No.2), are ascribed to the presence of QD2. Figure 4b shows the PL transients at different detection energies, which can be well fitted mono-exponentially. The spectral dependence of τ_d is plotted with solid circles in Figure 4a. The PL decay time at $E_{2,\max} = 1.284eV$ (600 ps) , lower than that at $E_{1,\max} = 1.347eV$ (700 ps), because of the higher probability of electron-hole wave-function overlap in the larger QDs[15]. For QD2, τ_d decreases slightly with increasing the emission energy, as expected. For QD1, however, τ_d increases first, reaches the maximum value of 708 ps at 1.346 eV, and then deceases with increasing the emission energies, quite different from that of the reference sample. This abnormal behavior is due to the carrier tunneling transfer from QD1 to

QD2, as discussed in detail below.

In 1996, Xie et al.[4] studied the pairing probability between the vertical InAs QDs, as a function of GaAs barrier thickness. In our case, the nominal barrier thickness between the QD1 and QD2 is around 60 MLs, resulting in a pairing probability as high as 70%.[4] The higher the QD1, the bigger the pairing probability. Moreover, the PL line shape of the QD ensemble is mainly determined by the size fluctuation of the QDs, especially the height distribution of the QDs in our case. The mean pairing probability of 70% means that nearly all of the QDs with emission energies lower than $E_{1,\max} = 1.347eV$, as shown in Region A of Figure 4a, are vertically aligned with the QDs in the second layer, which favors a tunneling transfer of carriers.

To evaluate the transfer time, we neglect the lateral tunneling between QDs in QD1, and use the averaged PL decay time ($\tau_R = 1050ps$) of the reference sample as reference. The tunnelling time τ_t for the QDs in the spectral region A of Figure 4a can then be calculated by the formula $1/\tau_d = 1/\tau_R + 1/\tau_t$, as shown in Figure 5. Using the correlation between the height distribution of QDs in Figure 1b and the PL line-shape of QD1 in Figure 4a, we can calculate the height of QDs in the first layer as a function of the emission energy by

$$(Height - Height_{mean}) / FWHM_{Height} = (E_{1,\max} - E) / FWHM_1 . \qquad (1)$$

The corresponding effective barrier thickness L_B will be $d_{spacer} - Height$, as seen in the cross-sectional TEM images in References 4 and 8. Then the tunneling time can be plotted as a function of L_B, as shown in Figure 5.

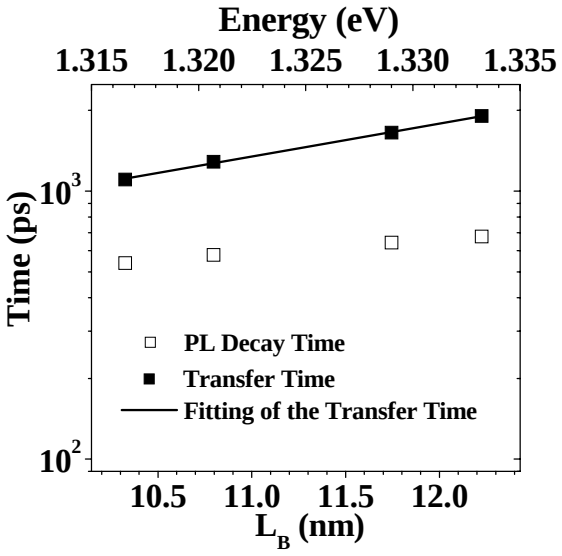

Figure 5 PL decay time and the tunneling time of the QDs in the Region A of Figure 4. The solid line is the least-squared fitting of the tunneling time.

According to the Wentzel-Kramers-Brillouin approximation, the dependence of the tunneling time τ_t on the barrier thickness is approximately written as

$$\tau_t \propto \exp[2L_B\sqrt{(2m^*/\hbar^2)(V-E)}], \qquad (2)$$

where m^* is the effective mass in the barrier, V is the band discontinuity of the conduction band, and E is the quantum level energy. The tunneling times in Figure 5 can be fitted by the straight line that follows (2), supporting that the observed dependence is caused by carrier tunneling. As the effective mass of holes is much larger that of electrons, the observed tunneling time is dominated by electron tunneling.

To compare our results with those published by other groups, we calculated the tunneling time as a function of $L_B\sqrt{m^*(V-E)}$, as shown in Figure 6. Here, we use the effective mass of electron in GaAs, $m^* = 0.067m_0$, m_0 is the electron mass. The value of the energy difference $V-E$ between the electron ground state in QD1 and the GaAs conduction band edge is calculated following the data in Ref. 16 and the emission energies of QDs shown in Figure 4. The least-squared fitting of the data with the formula, $\tau_t(ps) = t_0\exp[kL_B\sqrt{m^*(V-E)}[nm\sqrt{meV}]]$ gives $t_0 = 3.77, k = 0.175$ in this work, $t_0 = 8.24, k = 0.216$ in Tackeuchi et al.'s[6], $t_0 = 67.25, k = 0.103$ in Mazar's[7], and $t_0 = 3.103, k = 0.164$ in the $AlGaAs/GaAs$ asymetric double quantum well (QW) case of Wang et al.'s[16]. Obviously, our results are very close to the QW case, in both the magnitudes of tunneling rates and the slope. This indicates the non-resonant tunneling process could be the same for both the coupled QDs and QW. In the case of the coupled QWs, the tunneling assisted by longitudinal optical (LO) phonon emission is the most effective[17]. If non-resonant tunneling takes place only beteween the discrete QD states, the rate of LO phonon emission will be greatly decreased, due to so-called phonon-bottleneck effects. However, the phonon-bottleneck will break down if we consider the existence of quasi-continuum states blow the wetting layer states in SK QDs[18]. Therefore, our results suggest that the non-resonant carrier tunneling in the asymmetric bilayer QD structure takes place from the discrete state of QDs in QD1 and the continuum states of QDs in QD2, via LO phonon emission, as shown in Figure 7. After the excitation pulse, a lot of photo-generated carriers are captured by the QDs in both QD1 and QD2, the number of carriers in the discrete states of the QDs in QD1 will be decreased radiatively or through tunneling transfer to the continuum states of the QDs in QD2, via LO phonon

emission.

In summary, we demonstrated a new simple way of studying the vertical carrier tunneling transfer in an asymmetric bilayer InGaAs/GaAs QD structure, by using time-resolved photoluminescence. Our method is based on the correlation of the height distribution and the PL-line shape of QD ensembles, and the fact that the effective barrier thicknesses are modulated by the QD heights. The relationship between the tunneling time and the effective barrier thickness is found to be in agree well with the WKB approximation.

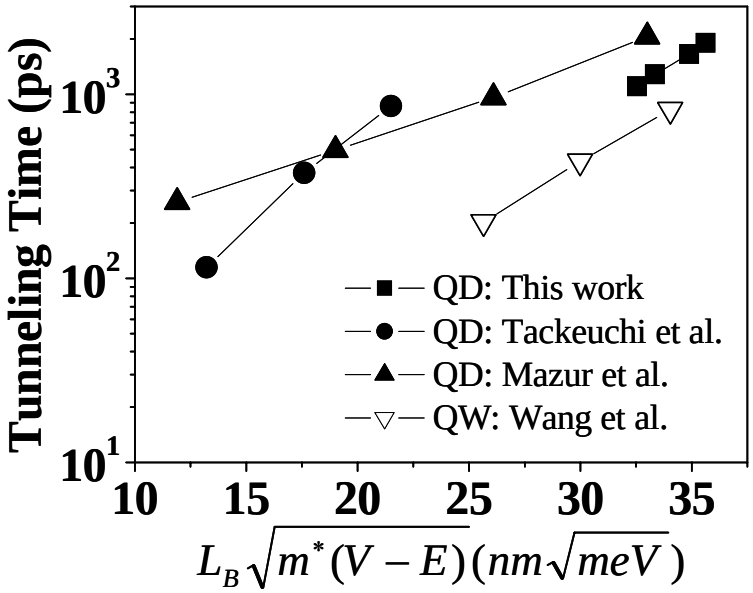

Figure 6 Tunneling time of the asymmetric bilayer QDs and QWs.

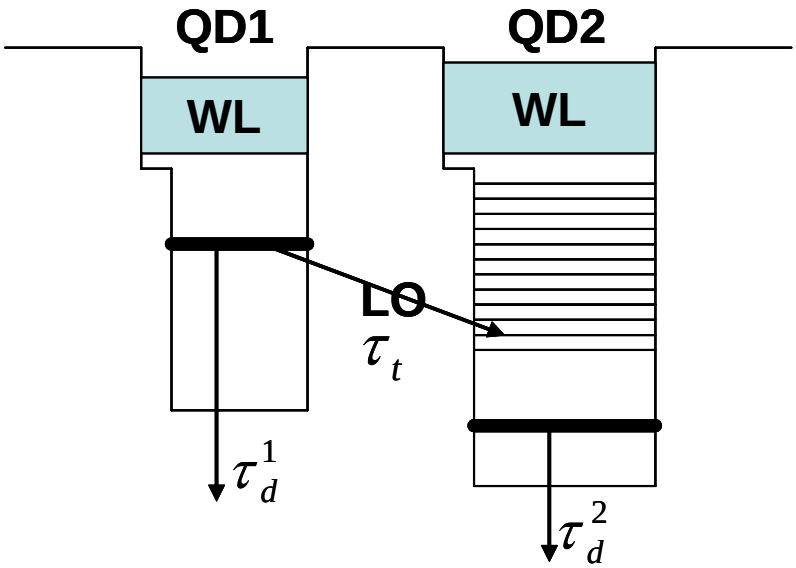

Figure 7 Schematic diagram of electron tunneling from the discrete states of the QDs in QD1 to the quasi-continuum states of QDs in QD2.

Zhangcheng Xu thanks Prof. Vadim Lyssenko and Prof. Dan Birkedal, for their assistant in time-resolved PL measurements. This work has been supported in part by the National Natural Science Foundation of China (Grant Nos. 60444010, and 60506013), the Danish Technical Science Research Council, the SRF for ROCS (SEM), the Startup fund for new employees of Nankai University, and the Marubun Research Promotion Foundation.

References

(1) Bimberg D.; Grundmann M.; Ledentsov N. N. *Quantum Dot Heterostructures*, Wiley, New York, **1999.**
(2) Konstantatos G.; Howard I.; Fischer A.; HooglandS.; Clifford J., Klem E.; Levina L.; Sargent E. H. *Nature* **2006**, 442, 180.
(3) Xu Z. C.; Birkedal D.; Juhl M.; Hvam J. M. *Appl. Phys. Lett.* **2004**, 85, 3259.
(4) Xie Q.; Madhukar A.; Chen P.; Kobayashi N. P. *Phys. Rev. Lett.*, **1996**, 75, 2542.
(5) Heitz R.; Mukhametzhano I.; Chen P.; Madhukar A. *Phys. Rev. B* **1998**, 58, R10151.
(6) Tackeuchi A.; Kuroda T.; Mase K.; Yoshiaki Nakata Y.; Yokoyama N. *Phys. Rev. B.* **2000**, 62, 1568.
(7) Mazur Yu. I.; Wang Zh. M.; Tarasov G. G..; Xiao M.; Salamo G. J.; Tomm J. W.; Talalaev V. *Appl. Phys. Lett.*, **2005**, 86, 63102.

(8) Suzuki Y.; Kaizu T.;Yamaguchi K. *Physica E* **2004** , 21, 555.
(9) Xu Z. C.; Birkedal D.; Hvam J. M.; Zhao Z. Y.; Liu Y. M.; Yang K. T.; Kanjilal A.; Sadowski J. *Appl. Phys. Lett.* **2003**, 82, 3859.
(10) Xu Z. C.; Leosson K.; Birkedal D.; J.M. Hvam; Sadowski J.; Zhao Z.Y.; Chen X.S.; Liu Y. M.; Yang K. T. *Journal of Crystal Growth* **2003** ,251,177.
(11) Birkedal D.; Leosson K.; Hvam J.M. *Phys. Rev. Lett.* **2001**, 87, 227401.
(12) Xu Z.C.; Zhang Y. T.; Hvam J.M.; Xu J. J.; Chen X. S.; Lu W. *Appl. Phys. Lett.* **2006**, 89, 13113.
(13) Mazur Yu. I.; Tomm J. W.; Petrov V.; Tarasov G. G.; Kissel H.; Walther C.; Zhuchenko Z. Ya.; Masselink W. T. *Appl. Phys. Lett.* **2001**, 78, 3214.
(14) Boggess T. F.; Zhang L.; Deppe D. G.; Huffaker D. L.; Cao C., *Appl. Phys. Lett.* **2001**, 78, 276.
(15) Horiguchi N.; Futatsugi T.; Nakata Y.; Yokoyama N.; Mankad T.; Petroff P. M. *Jpn. J. Appl. Phys. Part 1* **1999**, 38, 2559
(16) Wang T. H.; Mei X. B.; Jiang C.; Huang Y.; Huang J. M.; Zhou J. M.; Huang X. G.; Hai C. G.; Yu Z. X.; Luo C. P.; Xu J. Y.; Xu Z. Y. *Phys. Rev. Rev. B* **1992**, 46, 16160.
(17) Tackeuchi A.; Muto S.; Inata T.; Fuji T. *Appl. Phys. Lett.* **1991**, 58, 1670.
(18) Toda Y.; Moriwaki O.; Nishioka M.; Arakawa Y. *Phys. Rev. Lett.* **1999**, 82, 4114.